COBEM 2023 27TH INTERNATIONAL CONGRESS OF MECHANICAL ENGENEERING

ABCM Brazilian Society of Mechanical Sciences and Engineering
27th ABCM International Congress of Mechanical Engineering
December 04-08, 2023, Florianópolis-SC, Brazil

COB-2023-0893
PARTICLE SWARM OPTIMIZATION AND TIKHONOV REGULARIZATION FOR SOURCE IDENTIFICATION OF ATMOSPHERIC EMISSIONS OVER COMPLEX REGIONS

Roseane A.S. Albani
Instituto Politécnico, Universidade do Estado do Rio de Janeiro, Nova Friburgo, RJ - Brazil
roseanealves75@gmail.com

Juan P. L.C. Salazar
Engenharia Aeroespacial, Universidade Federal de Santa Catarina, Joinville, SC - Brazil
juan.salazar@ufsc.br

Vinicius V.L. Albani
Departamento de Matemática, Universidade Federal de Santa Catarina, Florianópolis, SC - Brazil
v.albani@ufsc.br

Davidson M. Moreira
SENAI-CIMATEC, Salvador, BA-Brazil
davidson.moreira@gmail.com

Antonio J. Silva Neto
Instituto Politécnico, Universidade do Estado do Rio de Janeiro, Nova Friburgo, RJ, Brazil
ajsneto@iprj.uerj.br

Abstract. *In this work we propose a source identification modelling that consists of the minimization of the Tikhonov regularization functional using the Particle Swarm Optimization technique. The objective function in the Tikhonov functional considers the discrepancy between the observed and numerical pollutant concentrations. The numerical concentrations are obtained as the solution of an adjoint advection-diffusion partial differential equation, jointly with a non-standard RANS k-ϵ turbulence model to provide the wind flow field. We perform the simulations using the CEDVAL wind tunnel experimental data A1-1 to provide the flow variables. The model implementation is performed within the framework of the CFD open-source code OpenFOAM and the commercial software Ansys Fluent and their results are compared. The proposed source estimation results were satisfactorily accurate.*

Keywords: *Source Identification, Particle Swarm Optimization, Computational Fluid Dynamics, Atmospheric Dispersion, OpenFoam, Ansys Fluent.*

1. INTRODUCTION

The source identification of atmospheric emissions is undoubtedly one of the most challenging subjects concerning atmospheric dispersion modelling. For emissions occurring over complex geometries, this task becomes even more difficult, since the pollutant cloud interacts with complicated structures of the local wind flow.

In many real-life scenarios, it is necessary to determine the origin of atmospheric pollutant emissions and other related parameters, such as the time of the releases, the amount of mass emitted, the source strength, etc. Whether a result of long-term industrial releases or accidental leakage, the characterization of atmospheric emissions is of great environmental importance. The estimation of relevant source parameters can be performed using a net of sensors that sample pollutant concentration, combined with meteorological monitoring data. However, obtaining accurate emission information with this procedure can be practically unfeasible, since a dense grid of sampling units would be necessary. A less expensive but effective alternative is to estimate the source parameters using inverse problem techniques from the measurements of a less dense array of sensors. This approach has received considerable attention in the last few decades. In addition to the environmental relevance of the problem, it is a challenging task owing to its intrinsic ill-posedness. Source identification models involve the coupled solution of forward and inverse problems. The forward problem usually considers an advection-diffusion partial differential equation (PDE), whose solution provides the pollutant concentration distribution. The atmospheric physical processes must be accounted for in the forward problem. These are usually included via boundary conditions, equation coefficients, and turbulence closure models. The main challenges for the source identifi-

cation methodologies are to develop a good representation of the forward problem and a technique to solve the resulting equations at a reasonable computational cost. In addition, the option for a methodology to solve the inverse problem is a relevant step to handle the aforementioned high ill-posedness of the source identification problem.

No technique offers optimal results in all possible situations. Thus, due to the relevance and difficulties underlying source identification problems, significant research has been dedicated to the development of methodologies for source estimation via inverse problems. The source identification approaches for considering releases underlying urban or other complex geometries generally use Computational Fluid Dynamics (CFD) to solve the forward model. Several researchers proposed source identification methodologies considering CFD-based dispersion models (Kumar *et al.*, 2015; Xue *et al.*, 2018). Concerning the inverse problem, the methodologies involved deterministic (Singh and Rani, 2015; Albani and Albani, 2019, 2020) or stochastic techniques (Addepalli *et al.*, 2011; Ma *et al.*, 2018; Albani *et al.*, 2021, 2023).

The proposed approach to address the source estimation problem is based on the Tikhonov-type regularization in combination with the stochastic Particle Swarm Optimization (PSO) method, yielding an efficient and robust estimation tool for urban-like environments. We apply an adjoint-state advection-diffusion PDE to provide the pollutant concentration distribution, which is solved only once, saving computational time. In addition, the non-standard k-epsilon model, appropriately designed to model atmospheric boundary layer (ABL) flow, proposed by Parente *et al.* (2011a), is applied as the turbulence closure model in the computation of the wind flow field. The model implementation is performed within the framework of the CFD open-source code OpenFOAM (Weller *et al.*, 1998) and the commercial software Ansys Fluent and their results are compared.

2. SOURCE IDENTIFICATION MODELING

In this work, we propose an inverse model to estimate the source location using a combination of an adjoint advection-diffusion PDE coupled with a non-standard k-ϵ turbulence model and the PSO technique. The estimation procedure consists of the minimization of an objective function using PSO. The objective function accounts for the discrepancy between the observed or experimental data and the numerical concentration distribution obtained from simulations. Next, we describe briefly these methodologies.

2.1 Inverse Modeling

To address the problem of estimating the source coordinates from observed concentrations, an inverse modelling technique is applied. Let C_{obs} denote the vector containing the set of experimental concentrations observed at each sensor position $\mathbf{x}_k = (x_k, y_k, z_k)$ with $k = 1, ..., n$, $\mathbf{x}_s = (x_s, y_s, z_s)$ denote the source coordinates, and $C^*(\mathbf{x}_s)$ stands for the solution of the adjoint dispersion model. Thus, we must find $\mathbf{x}_k$ such that

$$C_{\text{obs}}(\mathbf{x}_k) = C^*_k(\mathbf{x}_s), \quad k = 1, \ldots, n. \tag{1}$$

Equation (1) represents the so-called inverse problem (IP) of estimating the source location from observed concentrations. The IP is solved using Tikhonov's regularization, i.e., by finding the minimizers of the functional

$$\mathcal{F}(\mathbf{x}_s) = \| \ln(a + C_{\text{obs}}) - \ln(a + C^*)\|^2_{\ell_2} + 10^{-7}\|\mathbf{x}_s\|_{\ell_1}, \tag{2}$$

where a is a scalar constant to avoid zero arguments in the logarithmic function. The minimization of the functional $\mathcal{F}$ will be performed with the PSO. The PSO technique belongs to the category of swarm intelligence methods. It tries to emulate the social behaviour of flocks of birds and schools of fish from cognitive aspects considering the best position an individual ever had, besides the information exchange considering the best group position. The main objective of PSO is to provide information exchange between the group of individuals (or swarms) considering the aforementioned principles. PSO is considered a robust metaheuristic optimization algorithm with a simple computational implementation. The PSO accuracy is well documented, with applications in different problems arising in many areas of science and engineering. Moreover, they are simple to implement, with a vast number of pre-programmed codes available in different computing languages. For a precise description of these techniques, the reader can look for the references Camps Echevarría *et al.* (2019) and Gendreau and Potvin (2010).

2.2 Dispersion model

The solution of the following the PDE,

$$\mathbf{u} \cdot \boldsymbol{\nabla} C - \boldsymbol{\nabla} \cdot (K_{\text{eff}} \boldsymbol{\nabla} C) = Q(\mathbf{x})\delta(\mathbf{x} - \mathbf{x}_s), \tag{3}$$

provides the steady-state spatial distribution of a species concentration C for any position $\mathbf{x}$ over the computational domain Ω for a source located at $\mathbf{x}_s$. The vector $\mathbf{u}$ stands for the wind field given by the solution of the Navier-Stokes equations. Detailed information considering the wind flow and turbulence modelling can be found in the next subsection.

The diffusion coefficient K_{eff} is given by $K_{\text{eff}} = \mu/Sc + \mu_T/Sc_T$, where μ and Sc are the laminar viscosity and Schmidt numbers, respectively. The turbulent counterparts are denoted by μ_T and Sc_T. Further, Q stands for the emission rate and δ is the Dirac delta function. To complete the dispersion model in Eq. (3) the following boundary conditions are considered:

$$\mathbf{n} \cdot \boldsymbol{\nabla} C = 0 \quad \text{on the boundaries of } \Omega \text{ at } z = 0,\ z = H, \text{ and obstacle surfaces,} \tag{4}$$

$$C = 0 \quad \text{elsewhere (Ansys Fluent) and at the inlet (OpenFOAM),} \tag{5}$$

$$\mathbf{u} \cdot \boldsymbol{\nabla} C = 0 \quad \text{at the outlet (OpenFOAM).} \tag{6}$$

where the vector $\mathbf{n}$ stands for the outward normal of a given surface. Equation (4) assumes no flux across the corresponding boundaries, Eq. (5) indicates that the pollutant concentration goes to zero far away from the source of emission and Eq. (6) gives a convective outflow condition.

A usual procedure in source identification problems is to substitute Eq. (3) by an adjoint one Albani and Albani (2019). This procedure is performed to avoid solving the dispersion model in Eqs. (3)-(6) at each step of the PSO algorithm. The adjoint PDEs need to be solved only once, for each concentration measurement. Such a procedure results in significant savings in computational cost.

Considering the linearity of Eq. (3), it is possible to establish a direct relationship between the source and the sensors following the adjoint state PDE. Denoting the observed concentration at the k-th sensor by $C_{\text{obs}}(\mathbf{x}_k)$, it follows that,

$$C_{\text{obs}}(\mathbf{x}_k) = \int_\Omega C_k^* \mathcal{S} d\Omega = \langle C_k^*, \mathcal{S} \rangle, \tag{7}$$

wherein C_k^* represents the solution of the following adjoint-state PDE (Mamonov and Tsai, 2013):

$$-\mathbf{u} \cdot \boldsymbol{\nabla} C_k^* - \boldsymbol{\nabla} \left(K_{\text{eff}} \boldsymbol{\nabla} C_k^* \right) = \mathcal{S}_k, \tag{8}$$

wherein $\mathcal{S}_k$ represents the kth sensor, defined as

$$\mathcal{S}_k(x, y, z, t) = \delta(x - x_k)\delta(y - y_k)\delta(z - z_k),$$

where (x_k, y_k, z_k) is the spatial coordinate of the kth sensor location, considering a set of n sensors. The boundary conditions for Eq. (8) are identical to the ones given by Eqs. (4)-(6), by substituting C by C_k^* and, also switching the inlet/outlet boundary conditions.

2.3 Wind and turbulence modelling

This work applies the non-standard RANS k-ϵ turbulence model proposed by Parente *et al.* (2011a) to obtain the wind field by solving Eq. (8). It is assumed that before reaching the obstacle, the atmospheric flow occurs over a flat and homogeneous terrain with no changes in the meteorological conditions. In addition, no surface heat fluxes are considered, and the atmosphere is neutral. According to Richards and Hoxey (1993) an incompressible, horizontally homogeneous, stationary state, two-dimensional ABL flow can be described by the following hypotheses:

H.1 constant shear stress ,

H.2 null vertical component of the velocity,

H.3 constant pressure along the stream-wise (x) and the vertical (z) directions..

The $k-\varepsilon$ model consists of the transport equations for the turbulent kinetic energy (TKE or k) and the turbulent dissipation rate (TDR or ε). The aforementioned assumptions lead to equations for momentum, k and ε given respectively by

$$\mu_T \frac{\partial u}{\partial z} = \tau = \rho u_*^2 \ , \tag{9}$$

$$\frac{\partial}{\partial z}\left(\frac{\mu_T}{\sigma_k} \frac{\partial k}{\partial z} \right) + G_k - \rho\varepsilon = 0 \ , \tag{10}$$

$$\frac{\partial}{\partial z}\left(\frac{\mu_T}{\sigma_\varepsilon} \frac{\partial \varepsilon}{\partial z} \right) + \frac{\varepsilon}{k} C_{\varepsilon_1} G_k - \frac{\varepsilon^2}{k} \rho C_{\varepsilon_2} = 0 \ , \tag{11}$$

where $u_* \equiv \sqrt{\tau/\rho}$ is the friction velocity, C_{ε_1}, C_{ε_2}, σ_k, σ_ε, and C_μ are the model empirical constants defined originally by Launder and Spalding (1974). In addition, ρ is the air density, u is the wind velocity component in the x direction and μ_T is the turbulent viscosity. In the $k - \varepsilon$ model, the turbulent viscosity is defined as,

$$\mu_T \equiv \rho C_\mu \frac{k^2}{\varepsilon} \ . \tag{12}$$

Finally, the mechanical production of TKE term G_k is given by,

$$G_k = \mu_T \left(\frac{\partial u}{\partial z} \right)^2 \ . \tag{13}$$

In this work, we have implemented the modified $k - \epsilon$ model proposed by Parente *et al.* (2011a). This model is shortly outlined next. Assuming the equilibrium between production and dissipation in Eq. (10), we obtain the following expression for the TDR:

$$\varepsilon = k\sqrt{C_\mu}\frac{\partial u}{\partial z} \ . \tag{14}$$

By combining Eqs. (9), (12) and (14), we obtain a relation for C_μ,

$$C_\mu(z) = \frac{u_*^4}{k(z)^2} \ , \tag{15}$$

where the dependence on the z-coordinate has been made explicit. This variable $C_\mu(z)$ guarantees constant shear stress throughout the boundary layer and was first proposed by Gorlé *et al.* (2009).

The solution of equations (9)-(11) requires appropriate boundary conditions. Following Richards and Hoxey (1993), the inlet condition for velocity and TDR are given

$$u_{\log} = \frac{u_*}{\kappa} \ln\left(\frac{z + z_0}{z_0} \right) \ , \tag{16}$$

where κ is the von Kármán constant and z_0 is the aerodynamic roughness length. Combining the results from Eqs. (15), (14) and the analytical derivative $\partial u/\partial z$ from Eq. (16), we obtain a relation for ε,

$$\varepsilon = \frac{u_*^3}{\kappa(z + z_0)} \ . \tag{17}$$

Equation (17) is consistent with the velocity profile given by Eq. (16) and satisfies the requirement of equilibrium between production and dissipation of TKE within the ABL. However, to satisfy the TKE equation, the first term in Eq. (10) must be identically zero, i.e.,

$$\frac{\partial}{\partial z}\left(\frac{\mu_T}{\sigma_k}\frac{\partial k}{\partial z} \right) = 0 \ . \tag{18}$$

The solution of Eq. (18) considering Eqs. (12), (15) and the derivative of Eq. (16) respective to the z variable is given by

$$k = A \ln(z + z_0) + B \ , \tag{19}$$

where A and B are numerical constants that can be fitted to experimental data. The k inlet profile was previously proposed by Parente *et al.* (2011a). This set of inlet boundary conditions satisfies Eqs. (9) and (10). However, the substitution of Eqs. (9), (10)) and (14) in (11) results in an extra source term S_ε given by,

$$S_\varepsilon = \frac{\rho u_*^4}{(z + z_0)} \left[\frac{(C_{\varepsilon_2} - C_{\varepsilon_1})\sqrt{C_\mu}}{\kappa^2} - \frac{1}{\sigma_\varepsilon} \right] \ . \tag{20}$$

This term needs to be added to Eq.(11) to satisfy the equality.

To avoid the unintended stream-wise gradient in the flow variables, the default wall function formulations implemented in OpenFOAM and Ansys Fluent were also modified. The standard wall function implemented in Ansys Fluent was substituted by

$$u_p = \frac{u_*}{\kappa} \ln\left(\frac{z_p + z_0}{z_0} \right) \ . \tag{21}$$

In OpenFoam, the no-slip condition is set for the velocity at the wall and the wall adjacent centroid values are specified for ε, G_k, μ_T and k_p according to,

$$\varepsilon_p = \frac{u_*^3}{\kappa(z_p + z_0)} \ , \tag{22}$$

$$G_{k_p} = \frac{\rho u_*^3}{\kappa(z_p + z_0)} \ , \tag{23}$$

$$\mu_{T_p} = \rho u_* \kappa(z_p + z_0) \ , \tag{24}$$

$$k_p = A \ln(z_p + z_0) + B \ , \tag{25}$$

where the sub-index p indicates values evaluated at the first wall-adjacent cell centroid. These equations assume a constant stream-wise experimentally prescribed value of u_* and a prescribed value of k_p fitted from experimental data. They are consistent with the modelling assumptions made for the interior flow.

Finally, it is worth mentioning that we choose the model constant σ_ε such that the source term in Eq. (20) is identically zero at the wall adjacent cell centroid,

$$\sigma_\varepsilon = \frac{\kappa^2}{(C_{\varepsilon_2} - C_{\varepsilon_1})\sqrt{C_\mu(z_p)}} \ . \tag{26}$$

This step eliminates the need to define σ_ε.

In the flow region affected by the obstacle, the aforementioned formulation is not valid, since in this case hypotheses H.1-H.3 cannot be made and Eqs. (9)-(11) are no longer an adequate model for the flow. To circumvent this issue, an approach proposed by Parente *et al.* (2011a) that allows a gradual transition between the smooth and the disturbed ABL flow is used. The difference between the local velocity profile and the inlet profile defined by Eq. (16), $u_{\log}$, is considered by the introduction of the following blending parameter,

$$\Delta = \min\left[\left(\frac{u - u_{\log}}{u_{\log}}\right), 1\right] \tag{27}$$

As in Parente *et al.* (2011a), the source term S_ϵ and C_μ are then rewritten to provide a smooth transition between undisturbed and disturbed flow regime,

$$\phi = \phi_{\text{std}} + (1 - \Delta^\alpha)(\phi_{\text{hom}} - \phi_{\text{std}}), \tag{28}$$

where ϕ represents S_ϵ and C_μ. The subscripts hom and std designate the homogeneous values of these variables, given by Eq. (20) and (15) and the values for the standard $k - \epsilon$ model, namely $S_\epsilon = 0$ and $C_\mu = 0.09$, respectively.

2.4 Test problem

We now give a brief description of the problem to be solved in this work. We try to identify the spatial coordinates (x_s, y_s, z_s) from a single source numerical tracer experiment. The synthetic tracer experiment consists of one single source positioned at four different locations to produce different scenarios of concentration distribution. The sensors are positioned downstream of the obstacle at 0.035 m above the ground level. The y coordinate of the sensors varies between -0.05 and -0.3 m while the x coordinate assumes the values 0.1, 0.25, 0.5, 1.5 and 2 m. The relative position among source and sensors for the numerical tracer experiment are shown in Fig. 1. Figure 1 also shows the bottom of the computational domain. The computational domain is $\Omega = \{(x, y, z) \mid x \in [-1.05, 4.05],\ y \in [-0.3125, 0],\ z \in [0, 1.0]\ \text{m}\}$. Noise was added to emulate the experimental data sets according to,

$$C^{noise} = (1 + \zeta)C \ , \tag{29}$$

where $\zeta \sim N(0, 0.01)$. The numerical concentration C, given by the solution of Eq. (3) provide synthetic solution values sampled at the sensor position to be used in the source estimation process.

3. RESULTS

To evaluate the accuracy of the ABL modelling assumptions, we compared flow simulations with the CEDVAL A1-1 experiment (Leitl, 1998). The comparison for the longitudinal and vertical wind components, u and w respectively, as well as the TKE over different longitudinal positions, considering $y = 0$, are presented in Figs.2, 3 and 4. Overall, the results for the flow variables considering the simulation performed by OpenFOAM and Ansys Fluent are very similar to each other and in reasonable agreement with the experiment. The TKE overestimation by the k-ϵ model considering both OpenFOAM and Fluent simulations are greater near the obstacles as observed by Parente *et al.* (2011b). The model constants are presented in Tab. 1.

The source coordinates were estimated based on the minimization of the Tikhonov regularization functional given by Eq. (2) using the PSO technique. The PSO function code from the global optimization toolbox of MATLAB was used, with the following settings:

- Swarm size population of 100;
- *Self Adjustment Weight* = 1 and *Social Adjustment Weight* = 0.5;
- Inertial range of $[0.1, 1.2]$;
- Function Tolerance of 10^{-30}.

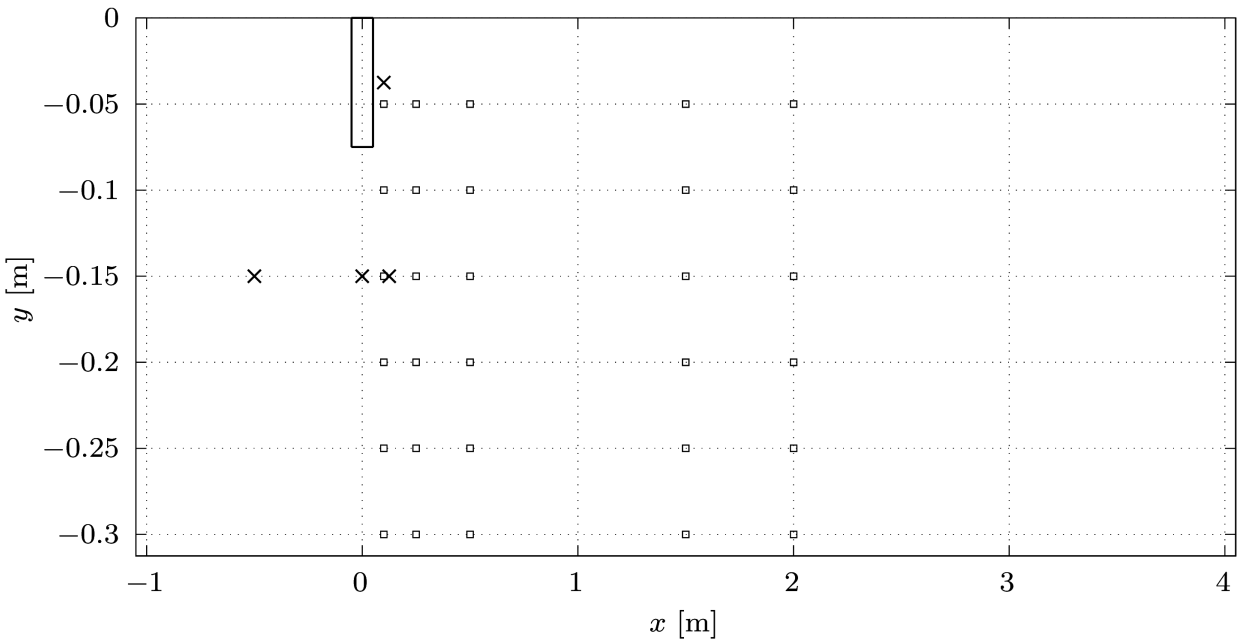

Figure 1. Representation of the numerical tracer experiment. Flow is from left to right. The empty rectangle represents the obstacle's horizontal dimensions. × Source position, □ sensor position.

Table 1. Model parameters. u_* and z_0 are obtained from the CEDVAL A1-1 experiment (Leitl, 1998). A and B are fitting parameters for the k inlet boundary condition (Eq. 19) obtained considering the CEDVAL datasets A1-1.

Parameter	Value	Units
u_*	0.377	m/s
z_0	0.0007	m
A	-0.0437	m^2/s^2
B	0.3548	m^2/s^2
κ	0.4892	-
C_{ε_1}	1.44	-
C_{ε_2}	1.92	-
σ_ε	1.9472	-
σ_k	1.0	-

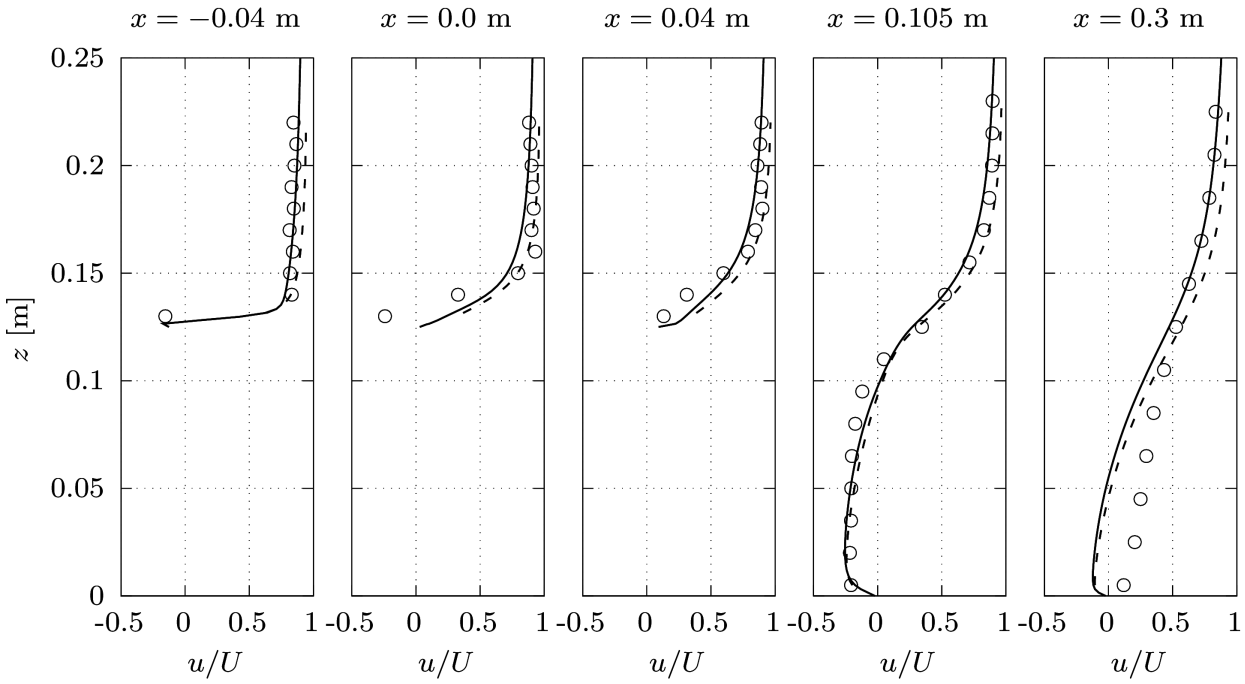

Figure 2. Normalized longitudinal wind component (u) along different downwind positions in the CEDVAL-A1-1 wind tunnel experiment. ○ Experiment, —— OpenFOAM, - - - - Fluent.

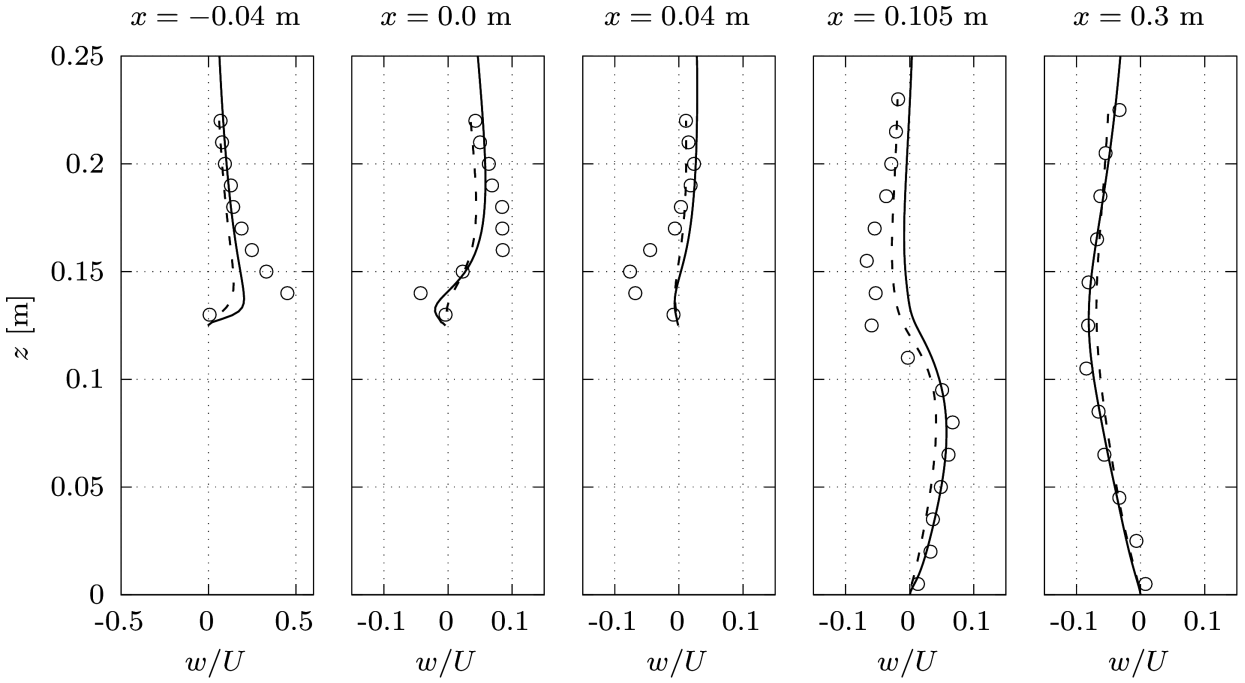

Figure 3. Normalized vertical wind component (w) along different downwind positions in the CEDVAL-A1-1 wind tunnel experiment. ○ Experiment, —— OpenFOAM, - - - - Fluent.

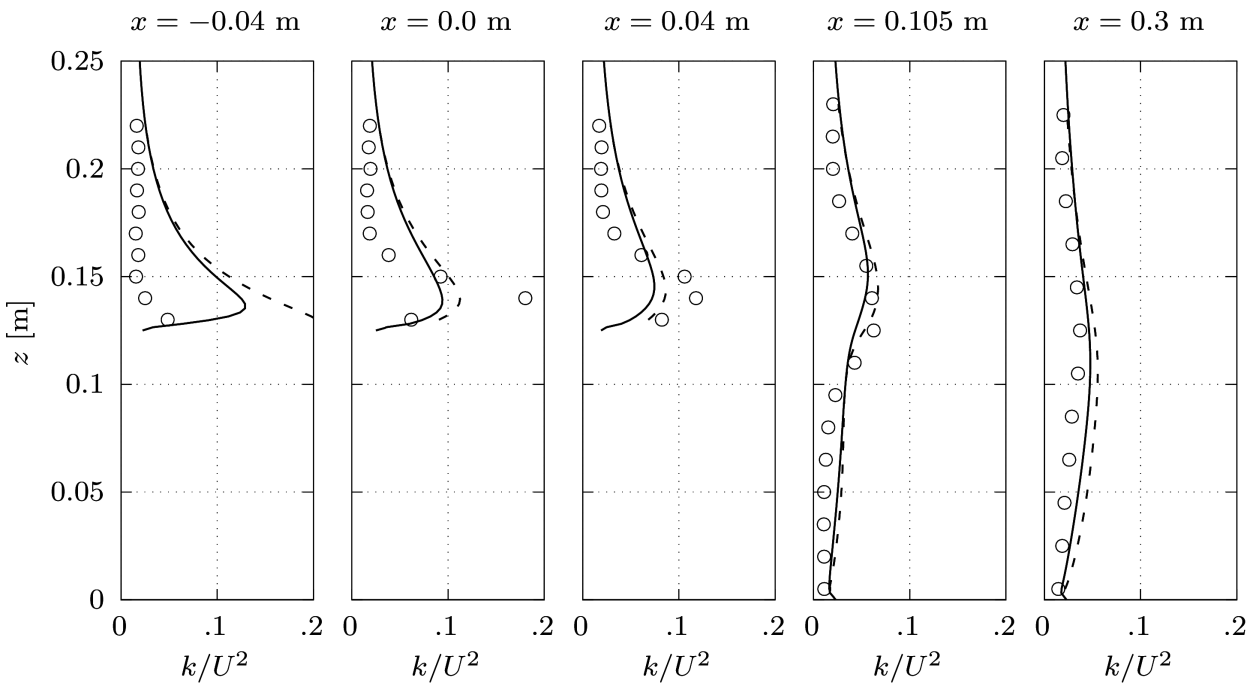

Figure 4. Normalized vertical TKE profiles along different downwind positions in the CEDVAL-A1-1 wind tunnel experiment. ○ Experiment, —— OpenFOAM, - - - - Fluent.

A similar setting to the PSO technique was applied previously in Albani *et al.* (2020). The PSO algorithm was used to perform the minimization a hundred times, to evaluate the solution sensitivity to the initial estimates. The solution of the adjoint PDE C_k^* was calculated for all 30 sensors. The minimization of the functional $\mathcal{F}$ (Eq. 2) was performed in two steps. First, consider the sampling points at rows 1, 2 and 3 and later for rows 2, 4 and 5, from left to right in the computational domain.

The results are presented as the median of the inverse problem solution. Figures (5) and (6) shows the source identification considering the rows of sensors for x $= 0.1,\ 0.25,\ 0.5$ m and x $= 0.25,\ 1.5,\ 2$ m respectively. The aim is to assess the inverse problem methodology using sets of sensors near and relatively far away from the sources. The results show that both OpenFOAM and Ansys Fluent performed satisfactorily. Considering the rows of sensors 1,2 and 3, OpenFOAM and Ansys Fluent solutions are very similar. For the farthest rows, 2, 5 and 6, OpenFOAM results seem to be slightly better. The underlying reasons for this require further investigation.

4. CONCLUSIONS

We modelled the inverse problem of atmospheric source location estimation using the Particle Swarm Optimization technique applied to the minimization of the Tikhonov regularization functional. A non-standard $k - \epsilon$ model coupled to an adjoint advection-diffusion PDE was applied to solve the forward problem. Although the well-known $k - \epsilon$ trend for the TKE overestimation near obstacles was confirmed, the proposed methodology found the source locations with satisfactory accuracy, especially for the OpenFOAM results of the forward problem. Despite efforts to model the problem the same in both Fluent and OpenFoam, they are different software. However, the reason why the OpenFOAM and Fluent results of the forward problem provided different trends in the inverse problem solutions needs further investigation.

5. ACKNOWLEDGEMENTS

R. Albani thanks Fundação Carlos Chagas Filho de Amparo à Pesquisa do Estado do Rio de Janeiro (FAPERJ) for the financial support through the grants E-26/202.932/2019 and E-26/202.933/2019. J. P. L. C. Salazar acknowledges the use of the computational resources of Laboratório de Computação Científica (LabCC) at Universidade Federal de Santa Catarina. AJSN acknowledges the financial support provided by SENAI CIMATEC, the Coordenação de Aperfeiçoamento de Pessoal de Nível Superior (CAPES) through the grants 88887.311757/2018-00 and 88887.194804/2018-00, the Conselho Nacional de Desenvolvimento Científico e Tecnológico (CNPq) through the grant 308958/2019-5, and the Fundação Carlos Chagas Filho de Amparo à Pesquisa do Estado do Rio de Janeiro (FAPERJ) through the grant E-26/200.899/2021CNE.

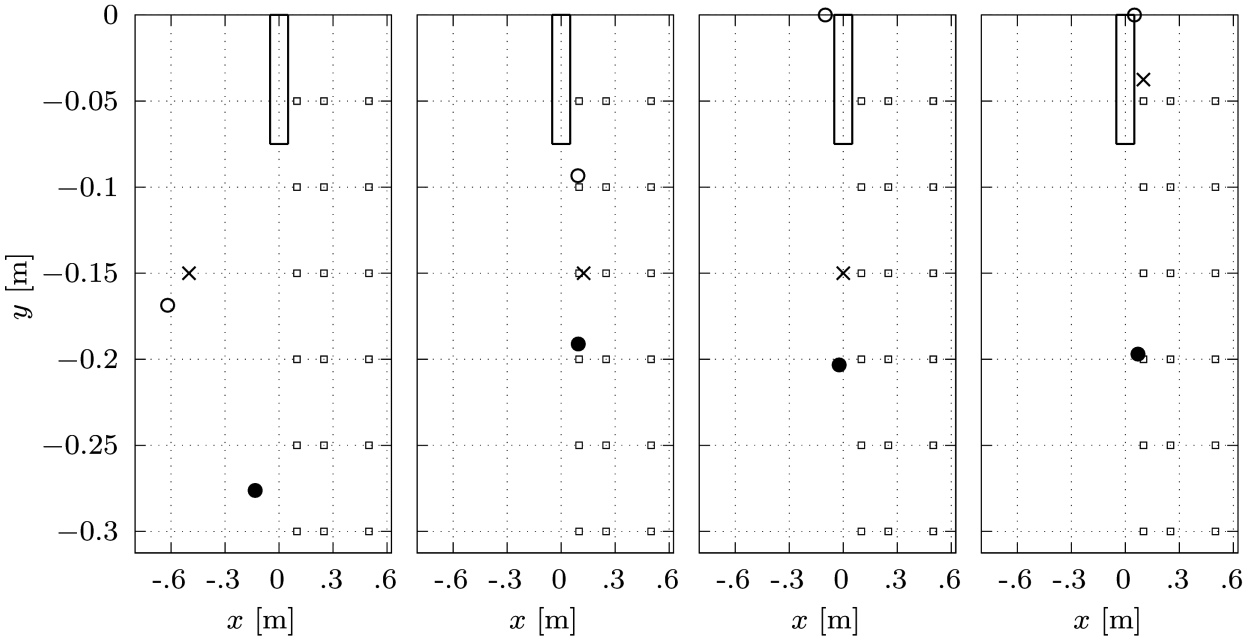

Figure 5. Source position estimation using PSO considering the forward problem obtained with OpenFoam and Fluent with sensor rows 1, 2 and 3. The black rectangle represents the obstacle position in the computational domain. × Actual source position, ○ OpenFOAM estimated source position, ● Fluent estimated source position, □ sensor position.

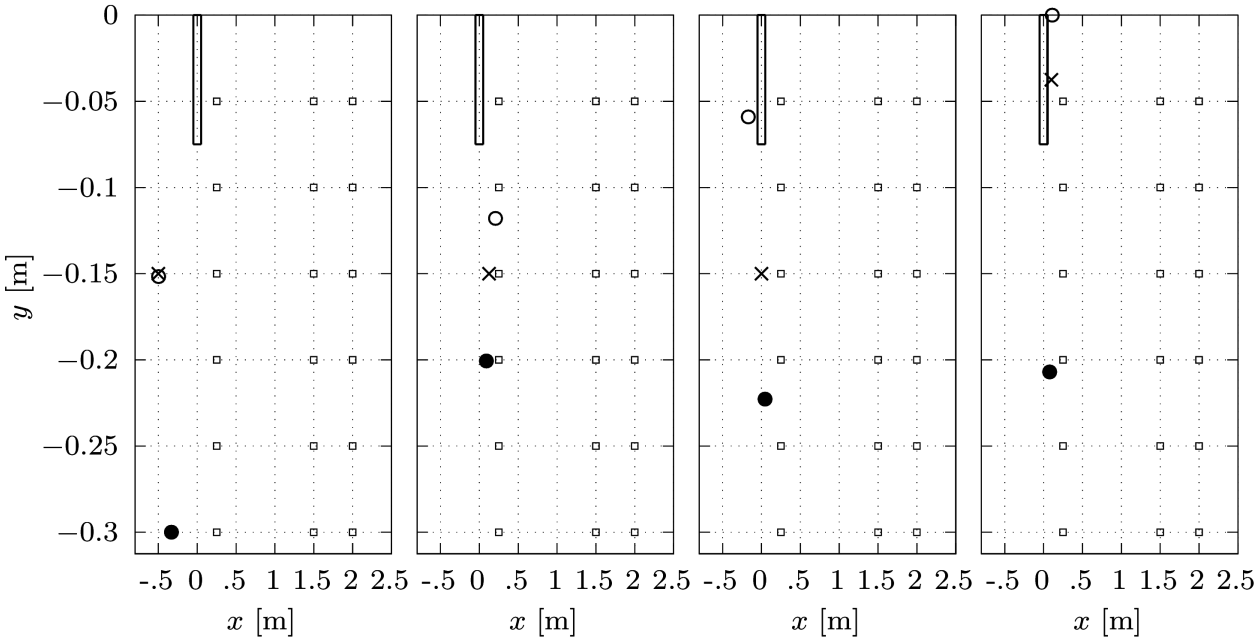

Figure 6. Source position estimation using PSO considering the forward problem obtained with OpenFoam and Fluent at rows 2, 4 and 5. The black rectangle represents the obstacle position in the computational domain. × Actual source position, ○ OpenFOAM estimated source position, ● Fluent estimated source position, □ sensor position.

6. REFERENCES

Addepalli, B., Sikorski, K., Pardyjak, E. and Zhdanov, M., 2011. "Source characterization of atmospheric releases using stochastic search and regularized gradient optimization". *Inverse Probl. Sci. Eng.*, Vol. 19, No. 8, pp. 1097–1124. doi:10.1080/17415977.2011.589901.

Albani, R. and Albani, V., 2020. "An accurate strategy to retrieve multiple source emissions in the atmosphere". *Atmos. Environ.*, Vol. 233, p. 117579. doi:10.1016/j.atmosenv.2020.117579.

Albani, R., Albani, V., Migon, H. and Silva Neto, A., 2021. "Uncertainty quantification and atmospheric source estimation with a discrepancy-based and a state-dependent adaptative MCMC". *Environ Pollut.*, Vol. 290, p. 118039. doi: https://doi.org/10.1016/j.envpol.2021.118039.

Albani, R., Albani, V. and Silva Neto, A., 2020. "Source characterization of airborne pollutant emissions by hybrid metaheuristic/gradient-based optimization techniques". *Environ Pollut.*, Vol. 267, p. 115618. doi: https://doi.org/10.1016/j.envpol.2020.115618.

Albani, R. and Albani, V., 2019. "Tikhonov-Type Regularization and the Finite Element Method Applied to Point Source Estimation in the Atmosphere". *Atmos. Environ.*, Vol. 211, pp. 69–78. doi:10.1016/j.atmosenv.2019.04.063.

Albani, R.A., Albani, V.V., Gomes, L.E., Migon, H.S. and Silva Neto, A.J., 2023. "Bayesian inference and wind field statistical modeling applied to multiple source estimation". *Environmental Pollution*, Vol. 321, p. 121061.

Camps Echevarría, L., Llanes Santiago, O., Campos Velho, H. and Silva Neto, A., 2019. *Metaheuristics for Optimization Problems*, Springer, chapter 3, pp. 43–83.

Gendreau, M. and Potvin, J.Y., 2010. *Handbook of Metaheuristics*. International Series in Operations Research and Management Science. Springer, 2nd edition.

Gorlé, C., van Beeck, J., Rambaud, P. and van Tendeloo, G., 2009. "CFD modeling of small particle dispersion: the influence of the turbulent kinetic energy in the atmospheric boundary layer". *Atmospheric Environment*, Vol. 43, pp. 673–681.

Kumar, P., Feiz, A., Singh, S., Ngae, P. and Turbelin, G., 2015. "Reconstruction of an atmospheric tracer source in an urban like environment". *J.Geophys.Res. Atmos.*, Vol. 120, pp. 12589–12604. doi:10.1002/2015JD024110.

Launder, B.E. and Spalding, D.B., 1974. "The numerical computation of turbulent flows". *Computer Methods in Applied Mechanics and Engineering*, Vol. 3, pp. 269–289.

Leitl, B., 1998. "Cedval at Hamburg University." <https://mi-pub.cen.uni-hamburg.de/index.php?id=432>.

Ma, D., Tan, W., Wang, Q., Zhang, Z., Gao, J., Wang, X. and Xia, F., 2018. "Application and improvement of swarm intelligence optimization algorithm in gas emission source identification in atmosphere". *J Loss Prevent Proc*, Vol. 56, pp. 262–271. doi:10.1016/j.jlp.2018.09.008.

Mamonov, A. and Tsai, Y.H.R., 2013. "Point source identification in nonlinear advection-diffusion-reaction systems". *Inverse Problems*, Vol. 29, No. 3, p. 035009. doi:10.1088/0266-5611/29/3/035009.

Parente, A., Gorlé, C., van Beeck, J. and Benocci, C., 2011a. "A comprehensive modelling approach for the neutral atmospheric boundary layer: Consistent inflow conditions, wall function and turbulence model". *Boundary-Layer Meteorology*, Vol. 140, pp. 411–428.

Parente, A., Gorlé, C., van Beeck, J. and Benocci, C., 2011b. "Improved k–ϵ model and wall function formulation for the RANS simulation of ABL flows". *Journal of Wind Engineering and Industrial Aerodynamics*, Vol. 99, No. 4, pp. 267–278.

Richards, P.J. and Hoxey, R.P., 1993. "Appropriate boundary conditions for computational wind engineering models using the $k - \epsilon$ model". *Journal of Wind Engineering and Industrial Aerodynamics*, Vol. 46, pp. 145–153.

Singh, S. and Rani, R., 2015. "Assimilation of concentration measurements for retrieving multiple point releases in atmosphere: A least-squares approach to inverse modelling". *Atmos. Environ.*, Vol. 119, pp. 402–414.

Weller, H.G., Tabor, G., Jasak, H. and Fureby, C., 1998. "A tensorial approach to computational continuum mechanics using object-oriented techniques". *Computers in Physics*, Vol. 12, No. 6, pp. 620–631. doi:10.1063/1.168744.

Xue, F., Kikumoto, H., Li, X. and Ooka, R., 2018. "Bayesian source term estimation of atmospheric releases in urban areas using les approach". *J. Hazard. Mater.*, Vol. 349, pp. 68–78. doi:10.1016/j.jhazmat.2018.01.050.

7. RESPONSIBILITY NOTICE

The authors are solely responsible for the printed material included in this paper.